JIPB Journal of Integrative Plant Biology

Research Article
https://doi.org/10.1111/jipb.13629

A widely targeted metabolite modificomics strategy for modified metabolites identification in tomato

Jun Yang[1,2†], Ridong Chen[1,2†], Chao Wang[1,2], Chun Li[1,2], Weizhen Ye[1,2], Zhonghui Zhang[1,2] and Shouchuang Wang[1,2*]

1. School of Breeding and Multiplication (Sanya Institute of Breeding and Multiplication), Hainan University, Sanya 572025, China
2. School of Tropical Agriculture and Forestry, Hainan University, Haikou 572208, China
†These authors contributed equally to this work.
*Correspondence: Shouchuang Wang (shouchuang.wang@hainanu.edu.cn)

Jun Yang

Shouchuang Wang

ABSTRACT

The structural and functional diversity of plant metabolites is largely created via chemical modification of a basic backbone. However, metabolite modifications in plants have still not been thoroughly investigated by metabolomics approaches. In this study, a widely targeted metabolite modificomics (WTMM) strategy was developed based on ultra-high performance liquid chromatography-quadrupole-linear ion trap (UHPLC-Q-Trap) and UHPLC-Q-Exactive-Orbitrap (UHPLC-QE-Orbitrap), which greatly improved the detection sensitivity and the efficiency of identification of modified metabolites. A metabolite modificomics study was carried out using tomato as a model, and over 34,000 signals with MS2 information were obtained from approximately 232 neutral loss transitions. Unbiased metabolite profiling was also performed by utilizing high-resolution mass spectrometry data to annotate a total of 2,118 metabolites with 125 modification types; of these, 165 modified metabolites were identified in this study. Next, the WTMM database was used to assess diseased tomato tissues and 29 biomarkers were analyzed. In summary, the WTMM strategy is not only capable of large-scale detection and quantitative analysis of plant-modified metabolites in plants, but also can be used for plant biomarker development.

Keywords: LC-MS, metabolic diversity, metabolite modificomics, modified groups, tomato

Yang, J., Chen, R., Wang, C., Li, C., Ye, W., Zhang, Z., and Wang, S. (2024). A widely targeted metabolite modificomics strategy for modified metabolites identification in tomato. J. Integr. Plant Biol. **00:** 1–14.

INTRODUCTION

Plants, which are sessile, synthesize a large and diverse range of compounds in order to adapt to complex and variable ecological environments (Weng et al., 2021). It is estimated that in nature plants produce a total of 200,000 to one million metabolites, far more than most other organisms (Saito and Matsuda, 2010; Afendi et al., 2012; Garagounis et al., 2021). This abundant chemical diversity is an important hallmark of the plant kingdom, with each individual plant containing from 5,000 to tens of thousands of metabolites, which can be divided into two main categories: primary metabolites and specialized metabolites (Fernie et al., 2004; Fang et al., 2019). The classes and structures of most primary metabolites are common and conserved in a variety of plants, providing not only the material basis of plant metabolism, but also a limited number of basic metabolic skeletons for the diversity of specialized metabolites. Common specialized metabolites mainly include terpenoids, alkaloids and phenylpropanoids; each class of metabolites shares the same metabolic skeleton (D'Auria and Gershenzon, 2005; Wang et al., 2019; Singh et al., 2023). These basic metabolic skeletons are further modified to form specialized metabolites with different structures varying in the nature, number, and binding positions of the modified groups. Primary metabolites can undergo a series of biochemical reactions (e.g., oxidation-reduction reactions) and/or different types of structural modifications (e.g., acylation, glycosylation, hydroxylation, isopentenylation and

methylation) to produce the complexity and diversity of plant specialized metabolites. Studies have shown that various modifications confer structural and functional diversity to proteins and metabolites. Protein modificomics focuses on its various post-translational modifications such as phosphorylation, acetylation, methylation, glycosylation, and so on (Reinders and Sickmann, 2007; Keenan et al., 2021). Similarly, metabolite modificomics is dedicated to resolving different modifications of the basic backbone of their molecular structure, and continued in-depth research in this field will provide many important insights into the diversity of plant metabolites (Wang et al., 2019). Glycosylation is considered to be one of the most important modification reactions for plant specialized metabolites, and glycosyltransferases are members of a multigene superfamily in plants that can transfer single or multiple activated sugars to a range of plant molecules, leading to the glycosylation of plant compounds (Zhang et al., 2022). However, new modification groups of plant metabolite structures still retain great unknowns, and there is a lack of overall systematic studies of various modifications in plants.

Structural modifications of metabolites, such as, glycosylation (Chen et al., 2020; Wang et al., 2020; Li et al., 2021), hydroxylation, malonylation (Ahmad et al., 2021; Xia et al., 2021), and methylation (Tieman et al., 2010; Yan et al., 2022), among other modifications that have been reported, not only have important effects on plant growth, development, and defense responses (Chen et al., 2020), but are also closely related to quality traits in crop plants such as coloration (Tanaka et al., 2008; Gandia-Herrero and Garcia-Carmona, 2013), flavor (Zhong et al., 2017; Wang, Qiang, et al., 2023), and nutrition (Zhu et al., 2018). In immature green tomato fruits, cholesterol is used as a precursor metabolite to synthesize tomatidine through a series of modifications including hydroxylation, oxidation, and transamination; tomatidine then undergoes four glycosylations to form the toxic substance α-tomatine, which protects the fruit from predation (Itkin et al., 2013; Sonawane et al., 2018). As the fruit ripens, α-tomatine is further acylated and glycosylated to form the non-toxic, non-bitter substance esculeoside A, which improves the nutritional and flavor quality of the tomatoes (Szymanski et al., 2020). In citrus fruits, flavanone 7-*O*-glucose is catalyzed by 1,2-rhamnosyltransferase or 1,6-rhamnosyltransferase to form bitter flavanone 7-*O*-neohesperidosides or non-bitter flavanone 7-*O*-rutinosides through different types of glycosylation reactions which affect fruit flavor (Frydman et al., 2004; Frydman et al., 2013). Anthocyanins are flavonoid pigments that are stabilized by glycosylation, methylation and acylation of the aglycone form (anthocyanidins) (Ono et al., 2006). In addition, all classical plant hormones have been found to exist in the form of glycosides (except ethylene) and to exhibit different biological activities in plants (Wang et al., 2019). For example, the main precursor of indole-3-acetic acid (IAA) is indole-3-pyruvic acid (IPyA); the glucosylation product of IPyA is involved in IAA homeostasis, as well as in the regulation of plant responses to environmental change (Chen et al., 2020). The glycosylation product of indole-3-butyric acid (IBA) is involved in cotyledon development and flowering regulation in Arabidopsis (Zhang et al., 2016).

Liquid chromatography-mass spectrometry (LC-MS) is a powerful technique for the separation of compounds, with high sensitivity and a wide detection range (Tolstikov and Fiehn, 2002; De Vos et al., 2007), and the use of LC-MS for targeted, untargeted, pseudotargeted, and widely targeted metabolomic assays has been proposed for the detection of compounds in complex samples (Chen et al., 2013; Shi et al., 2017; Lv et al., 2020; Zheng et al., 2020). In particular, a widely targeted metabolomics strategy based on ultra-high performance liquid chromatography-quadrupole/linear ion trap (UHPLC-Q-Trap; Chen et al., 2013) has been applied to metabolomic analyses of crops such as citrus (Shen et al., 2023; Wang, Shen, et al., 2023), maize (Wen et al., 2014), rice (Fang et al., 2021; Yang et al., 2022), and tomato (Zhu et al., 2018). However, this approach, although capable of capturing large-scale metabolic signals, cannot effectively target modified metabolic signals and resolve their molecular structures. An untargeted modification-specific metabolomic approach based on in-source collision-induced dissociation (ISCID) LC-high-resolution MS (LC-HRMS) can specifically target modified metabolites; using this approach, a total of 910 metabolite signatures, including of acetylation, glucose glycosylation, glucuronidation, ribose coupling, and sulfation, were detected in urine from healthy subjects and patients with cirrhosis (Dai et al., 2014). This method was also applied to tea tree samples, and a total of 144 glycosidic substances were identified (Dai et al., 2016). More recently, a nontargeted method for the detection of modified metabolites based on HRMS has been developed (Li et al., 2019); this method was applied to perform an unbiased analysis of 13 types of modified metabolites in urine (Li et al., 2019). Another method, combining glycosides-specific metabolomics and precursor isotopic labeling, can efficiently and accurately identify glycosylated products in plants, including those of glycosylation modifications (Wu et al., 2022). However, all assays developed to date only target a few types of metabolite modifications or known metabolite modifiers. Non-target-based assays are unable to detect new modified metabolites at ultra-low micro levels due to low sensitivity, while target-based assays can only detect known metabolic modifiers but not new ones. However, although these methods can be used to increase the number of structural modifications detected, the comprehensive detection of all modification types in a sample remains inaccessible and it is difficult to uncover new modified metabolites.

In this study, we combined UHPLC-Q-Trap and UHPLC-Q-Exactive-Orbitrap (UHPLC-QE-Orbitrap) to develop a widely targeted metabolite modificomics (WTMM) strategy that enables high-throughput identification and highly sensitive quantification of modified metabolites. A stepwise neutral loss-enhanced product ion (stepwise NL-EPI) method based on UHPLC-Q-Trap was used to detect possible modified metabolic signals in plants, followed by structural annotation

using HRMS information collected by UHPLC-QE-Orbitrap. A tomato metabolite modificomics database was constructed and 125 modification types and 2,118 annotated metabolites of tomato were identified, of which 165 modified metabolites were newly identified in this study. Finally, the WTMM strategy was used to compare the differences in metabolic profiles of tomato after infection with *Ralstonia solanacearum* and to screen 29 marker metabolites.

RESULTS

Overview of the WTMM strategy

To systematically explore the diversity of plant metabolite types and structures, a WTMM strategy based on UHPLC-Q-Trap and UHPLC-QE-Orbitrap was developed (Figure 1; Table S1). First, to obtain metabolic profiles of various modified metabolites, a new method of stepwise NL-EPI based on UHPLC-Q-Trap was developed. NL values were set from 14 to 245 Da, where the mass step was 1.0 Da, and the scan range of the corresponding precursor ions for each NL transition was set from 19 to 1,000 Da (Figure 1A). For example, glycosylation is one of the most common structural modifications in plants, and the NL value for hexosylation of glucose and galactose is 162 Da. Compared with the QE-Orbitrap-based full MS/dd-MS^2 mode, the Q-Trap-based stepwise NL-EPI method can obtain a richer metabolic signal when detecting hexosylation modifications (NL value = 162 Da). The former detected 326 neutral loss signals while the latter detected 460, which is 41% more in number, and both detected very few overlapping signals, accounting for only 7.2% of the total signal (Figure 1A). Thus, the WTMM strategy integrates the advantages of high sensitivity and wide coverage of Q-Trap and high resolution of QE-Orbitrap to detect a wider range of metabolites.

Second, in order to accurately annotate metabolic signals in the MS2 spectral tag (MS2T) library (Chen et al., 2013), HRMS data and algorithms were integrated for structural elucidation of the modified metabolites. Details of the criteria for metabolite structure identification are given in the "Materials and Methods" section. For example, the molecular formula of the metabolic signal NL35146 in the MS2T library was calculated as C23H42NO7P according to the accurate m/z. Further analysis identified neutral losses of NL = 141.0201 (phosphoryl-ethanol group) and NL = 215.0560 (glycerol-phosphoryl-ethanol group) in the fragmentation pattern of its mass spectrum. Finally, the metabolic signal was identified as PE 18:3 by comparing MS2 information with standard and commercial metabolic databases (Figure 1B). Note that the annotation of metabolic signals can be challenging due to the large number of modification profiles obtained using the WTMM approach. Therefore, in this study, the MS2 Analyzer software was used to automatically identify the NL of metabolic signals (Figure S1) and obtain modification group information to further improve the MS2T library. In addition, MetDNA identification algorithms were used to construct metabolic networks containing both known and unknown signals (Figure S2A–C), and many metabolites were annotated, including lycopene-related pathways (Figure S2D).

Third, to obtain stronger and more accurate metabolic signals, a pipeline was developed for transition selection and optimization of MS parameters. For example, for the precursor ion m/z of 476.3 Da, two high abundance fragment ions (Q3) were selected from the MS2T library and combined with the parent ion to form two candidate transition pairs (476.3/335.1 and 476.3/304.1). The above transitions were then quantitatively analyzed using the scheduled multiple reaction monitoring (sMRM) scanning mode, where declustering potential (DP) and collision energy (CE) were set to 10, 20, 30, 40, 50, and 60 orthogonally combined into 36 sets of test parameters. Unqualified chromatographic peaks with poor peak shape, low signal intensity or low signal-to-noise ratio, and/or overly high signal intensity and peaks were removed; good chromatographic peaks were retained and corresponding detection parameters were recorded for subsequent analyses (476.3/304.1, DP = 30, CE = 20) (Figure 1C).

Construction of a WTMM database for tomato

In this study, the WTMM strategy was used to detect mixed samples composed of different tomato tissues (i.e., leaves and roots) (Table S2); the collected metabolic signals were screened (signal-to-noise ratio > 10) and redundant. More than 34,000 high-quality metabolic signals were obtained with MS2 information from 232 NL transitions (Table S3), and these were combined to form a tomato metabolite modificomics MS2T library. This library included a large number of modified metabolic profiles with high resolution acquired based on QE-Orbitrap, as well as new metabolic signals that could only be detected based on Q-Trap in different NL types (only new signals are shown) (Figure 2A, B).

To facilitate the identification and annotation of metabolic signals, a total of 240 modified metabolites were annotated by first comparing the m/z, retentiontime (RT), fragmentation pattern, and NL motifs obtained with standards (Table S4). The metabolites identified included pyridoxal 5′-phosphate (NL06838, $m/z = 248.0$, RT = 1.15, NL = 98, phosphorylation), *p*-coumaroylagmatine (NL08700, $m/z = 277.1$, RT = 2.50, NL = 146, *p*-coumaroylation), *O*-glucosyl-tomatidine (NL23577, m/z = 578.3, RT = 4.50, NL = 162, anhydrohexose conjugation) (Figure 2C).

For metabolic signals lacking standards, metabolites were identified using metabolic databases and literature searches. MS2 Analyzer was used to automate the identification and characterization of NLs in MS2T; a total of 2,878 modification groups were identified, greatly improving the MS2T library (Table S5). As an example, the RT of metabolic signal NL23615 was 5.03 min, indicating that it is a moderately polar compound; its MS2 data contained the characteristic peak of tricin 331.4 Da, which is presumed to be a flavonoid with tricin as the basic skeleton. The NL analysis revealed that the MS2 information contained fixed mass differences of 86 and

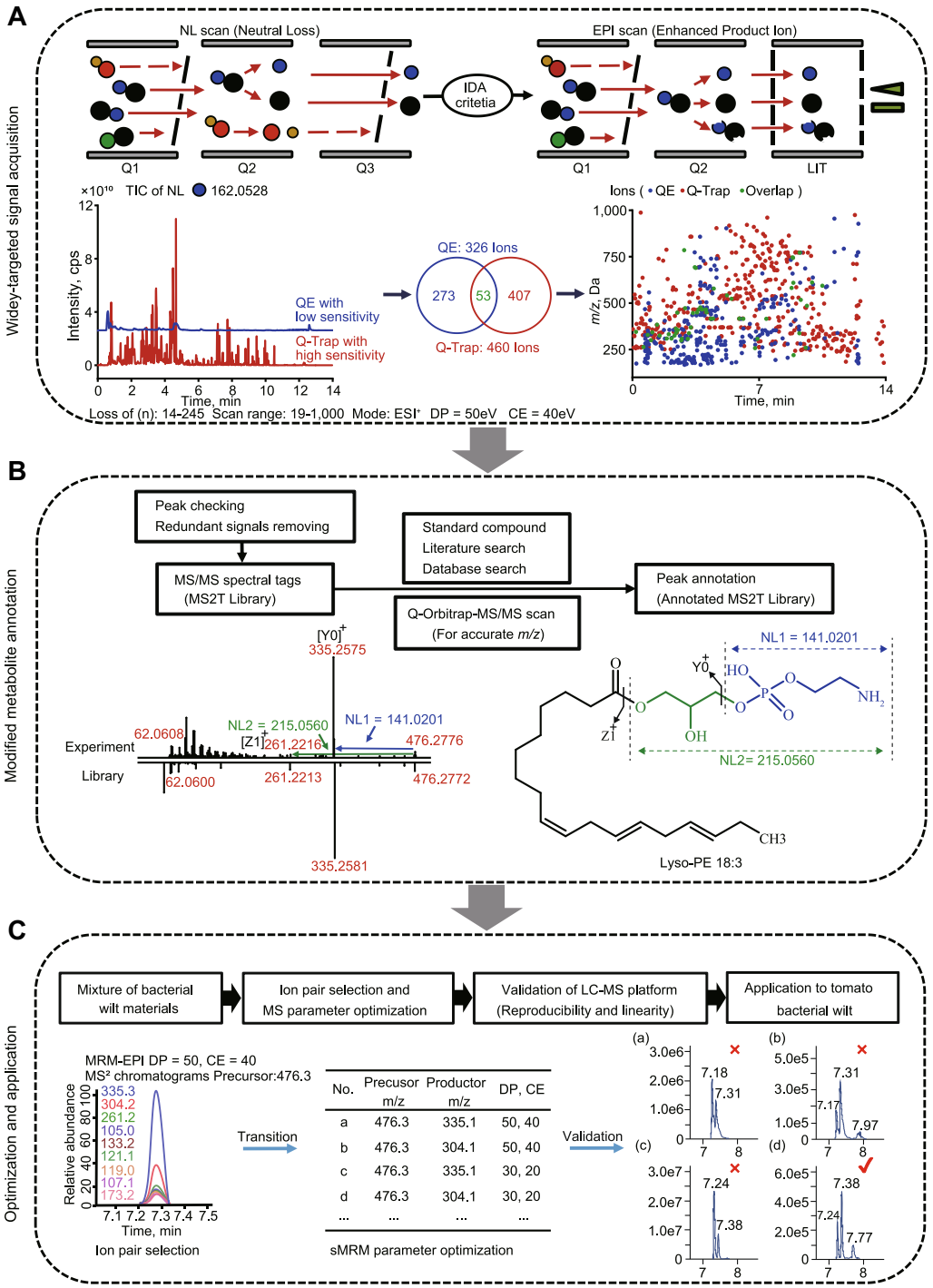

Figure 1. The main procedures for WTMM strategy

(A) High-throughput acquisition of modified metabolite profiling by ultra-high performance liquid chromatography-quadrupole-linear ion trap (UHPLC-Q-Trap) in stepwise NL-EPI scanning mode. The NL value ranged from 14 to 245 Da, with precursor ion scanned from 19 to 1,000 Da, and the DP and CE in positive ion mode were set to 50 eV and 40 eV, respectively. **(B)** Annotation of MS2 spectral tag (MS2T) library based on high-resolution mass spectrometry data from UHPLC-Q-Exactive-Orbitrap (UHPLC-QE-Orbitrap). The green and blue arrows in the mass spectrum represent NL transitions, corresponding to the modified groups in the structural formula. **(C)** Optimization of the main parameters of the WTMM strategy; (a, b) fail: convolution of peaks; (c) fail: peak intensity exceeds threshold (peak area > 1−E7); (d) pass: single peaks without convolution and intensities between 1−E5 and 1−E7. Chromatographic peaks are shown in a cartoon schematic (see the "Materials and Methods" section for screening process details). CE, collision energy; DP, declustering potential; EPI, enhanced product ions; NL, neutral loss; sMRM, scheduled multiple reaction monitoring; TIC, total ion chromatography; WTMM, widely targeted metabolite modificomics.

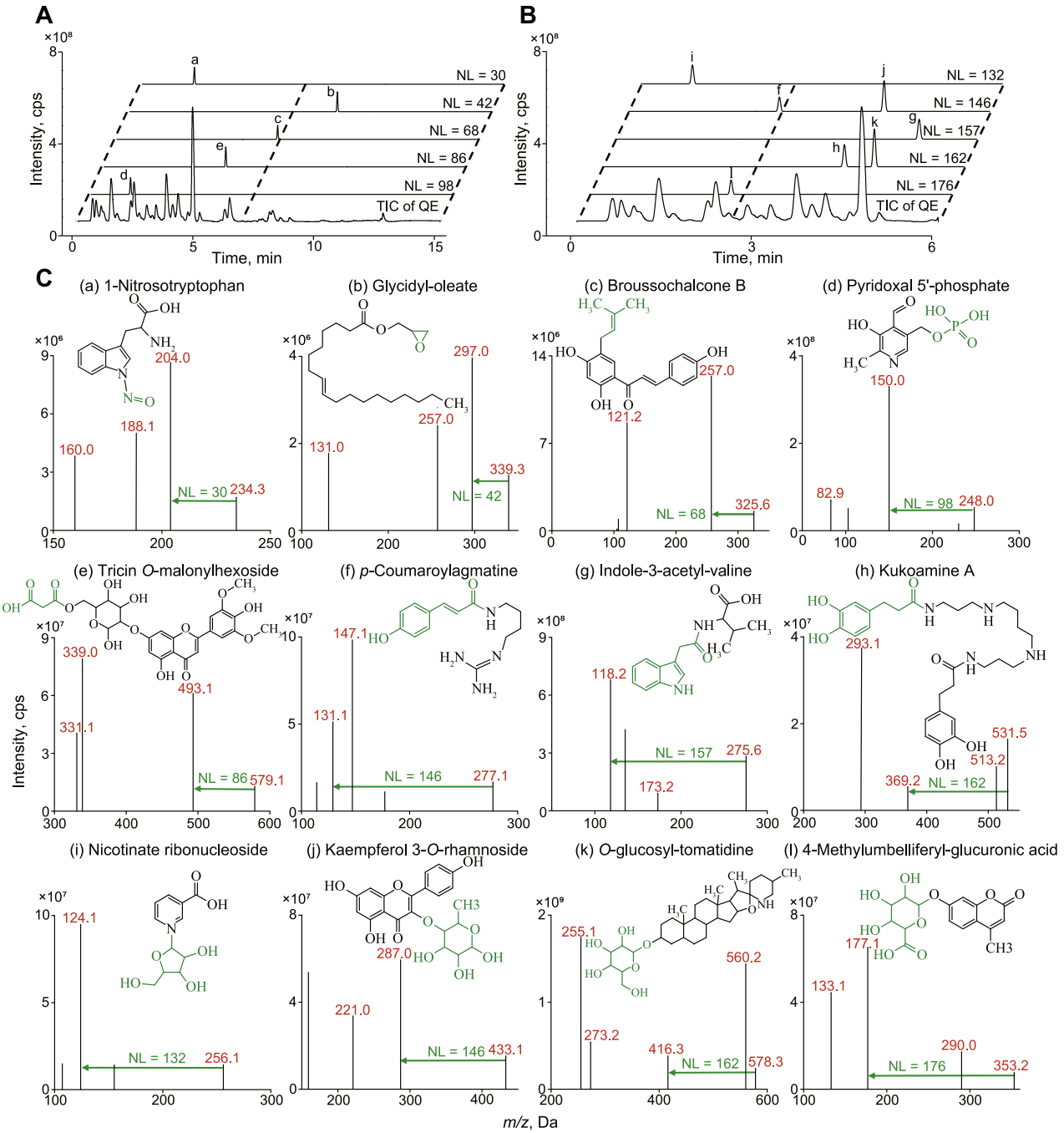

Figure 2. Identification and annotation of modified metabolites in tomato

(A, B) Novel chromatographic peaks detected via the quadrupole-Exactive-Orbitrap (QE-Orbitrap) and quadrupole-linear ion trap (Q-Trap) approach. Comparison of chromatograms for retention times of 15 min **(A)** and 6 min **(B)** The TIC based on QE-Orbitrap in full mass spectrometry (MS) scanning mode, and the other chromatograms show only new peaks corresponding to specific modified groups detected by the Q-Trap approach. **(C)** The structures and MS2 spectra of the modified metabolites. Green arrows represented NL transitions, corresponding to the modified groups in the structural formula. NL, neutral loss; TIC, total ion chromatography.

162 Da, which are typical of malonyl and hexosyl, respectively. In addition, MetDNA was also used to support metabolite identification, and a total of 886 metabolic signals were annotated with MetDNA (Table S6). In total, more than 1,700 metabolites were annotated, including alkaloids, amino acids, flavonoids, lipids, phenolamines, and phytohormones.

A total of 165 novel modified metabolites reported in tomato were identified in the above analysis, including S-[2-(2-pyridinyl) ethyl] cysteine (NL 77.0294, pyridinylation), 3-(2-acetamidoethyl)-1H-indol-5-yl hydrogen sulfate (NL 79.9935, sulfation), 2-hydroxycyclohexyl-1-phenylethanone (NL 98.0728, hydroxycyclohexylation) (Figure S3). Ten types

of structural modifications in glycerol phospholipids such as PE 18:3 (NL 141.0201/215.0506, glycerol-phosphoryl-ethanol ammoniation) were further analyzed (Figure S3; Table S4). Meanwhile, 21 typical structural modifications were summarized for the flavonoid metabolites in tomato. These were classified into five major categories according to the structural characteristics of the modification groups: carbon chain modification, single glycosylation modification, multiple glycosylation modification, acyl-glycosylation modification and other modification types (Figure S4). Using the WTMM approach, a tomato database covering 125 modification types and 2,118 metabolites was established (Tables S4, S7).

Comparison and evaluation of quantitative methods based on Q-Trap and QE-Orbitrap in WTMM strategy

To systematically evaluate the strategy developed in this study, the tomato WTMM database was used to perform modified metabolic profiling in mixed tissue samples from *R. solanacearum*-infected tomato. Plant phytohormones are usually present at very low levels; therefore, gibberellin detection was used to assess the sensitivity of the method. Gibberellin A4 (GA4) was detected in the Q-Trap-based stepwise NL-EPI method at NL = 131 Da (NL12452, unknown modification), and the metabolite detected determined via comparison with a standard. However, no signal peak was detected in the same sample using the QE-Orbitrap-based full MS/dd-MS2 mode (Figure 3A), indicating that Q-Trap approach has better sensitivity for quantitative analysis in the WTMM strategy. Meanwhile, five concentration gradients (0.25, 0.5, 1, 1.5, 2 μg/mL) of GA4 standards were detected using the Q-Trap approach, and the GA4 standard curve was plotted for absolute quantification (Figure 3B). Correlation coefficients (R^2) were greater than 0.99, indicating that the standard curve was in good agreement with the original datatype.

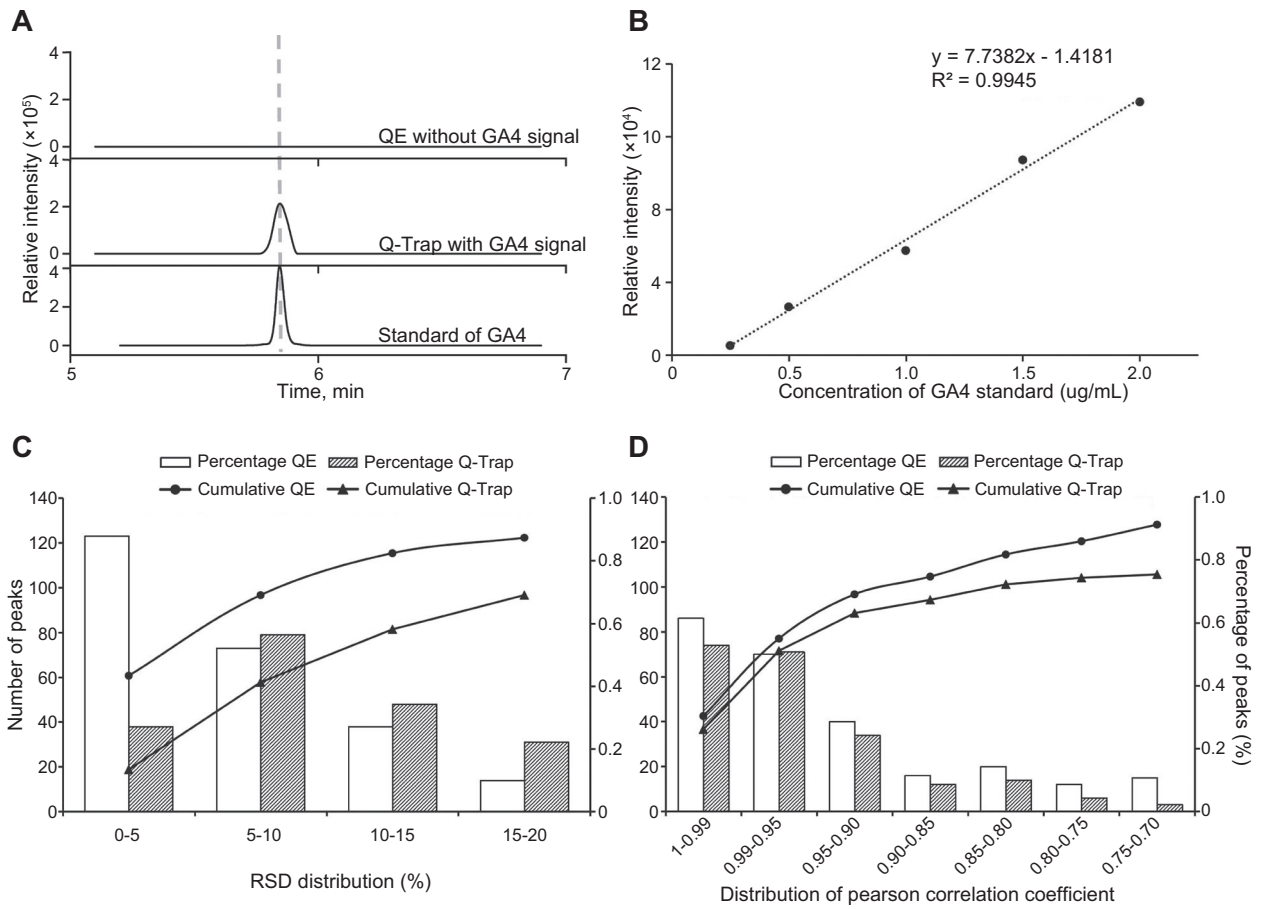

Figure 3. Evaluation of the WTMM strategy

(A) Evaluation of the sensitivity of the WTMM strategy. The gibberellin A4 (GA4) content in tomato tissues was determined based on different detection methods. The extracted ion current map (XIC) obtained by the quadrupole-linear ion trap (Q-Trap) and the quadrupole-Exactive-Orbitrap (QE-Orbitrap) method for the detection of gibberellin (GA4). **(B)** Standard curve of GA4. GA4 standards at different concentrations (0.25, 0.5, 1, 1.5, and 2 μg/mL) were scanned using MRM mode, and standard curves drawn using chromatographic peak area data. **(C)** Evaluation of the reproducibility of the Q-Trap approach. Ten identical quality control (QC) samples were tested using both methods, and the peak area data were extracted from dataset for relative standard deviation (*RSD*) calculations. **(D)** Evaluation of linearity of the Q-Trap approach. A concentration gradient (0.083, 0.1, and 0.125 g/mL) of QC samples were analyzed using both methods, and the chromatographic peak area data were extracted from each dataset for Pearson correlation coefficient calculation. MRM, multiple reaction monitoring; WTMM, widely targeted metabolite modificomics.

The acquired metabolic signals were subsequently screened using the MS parameter optimization strategy in Figure 1C, and a total of 826 substances with high-quality metabolic signals were screened for detection in subsequent experiments. The 284 metabolic signals were identified using the WTMM strategy by comparing the precursor ions, retention times and MS fragmentation data for each signal (Table S8). These 284 peaks were then used to compare the quantitative analysis ability of both Q-Trap and QE-Orbitrap methods. First, to compare detection reproducibility, ten replicate quality control (QC) samples were scanned simultaneously using both methods; peak area data for the 284 outgoing peaks in each dataset were extracted and the relative standard deviation (*RSD*) calculated separately for each (Figure 3C). For the Q-Trap approach, the *RSD* values for 43% and 69% of the detected metabolites were less than 5% and 10%, respectively; meanwhile, only 13% and 41% of the QE-Orbitrap-detected metabolites had *RSD* values less than 5% and 10%. These results indicate that the Q-Trap approach had greater reproducibility.

Next, the linearity of the two detection methods was evaluated. Compared to the QE-Orbitrap platform (full MS/dd-MS2 mode) which scans the entire *m/z* range, the Q-Trap platform (sMRM mode) detects only defined metabolites, the detector is less prone to saturation and has a wider linearity range. A concentration gradient (0.083, 0.1, and 0.125 g/mL) of QC samples was set up in triplicate and injected for detection with both methods. The peak areas corresponding to each sample were extracted and averaged, and linearity assessed using Pearson's correlation coefficients (Figure 3D). The correlation coefficients differed significantly between the two methods: for example, 91% (Q-Trap) versus 75% (QE-Orbitrap) of the metabolites had correlation coefficients greater than 0.70, and 30% (Q-Trap) versus 26% (QE-Orbitrap) of the metabolites had correlation coefficients greater than 0.99. Therefore, the Q-Trap approach has a wider linearity and is more suitable for metabolomic analysis of complex biological samples. Overall, the Q-Trap approach outperformed QE-Orbitrap in terms of sensitivity and quantitation, achieving large-scale detection and quantitative analysis of modified metabolites in plants.

Screening differentially accumulated metabolites in response to tomato bacterial wilt

To test the applicability of WTMM strategy for detection of modified metabolites in plant samples, the optimized WTMM database was used to screen differential metabolites in response to tomato blight. Metabolites were extracted from 60 diseased and healthy tomato tissue samples (see the "Materials and Methods" section), and peak areas for the 826 substances detected were obtained for subsequent statistical analysis (Table S9).

Principal component analysis (PCA) was used as an unsupervised method to investigate the differences in metabolic profiles between healthy control and *R. solanacearum*-infected groups in different tissues of tomato. Principal component analysis results showed significant separation of four different groups of material, which reflected significant differences in metabolite levels in different tissues, with 52.2% of the differences explained by the first two principal components (36.3% for PC1 and 15.9% for PC2). In addition, the leaf control (LC) and leaf disease (LD) materials were clearly separated in the PCA, while the root control (RC) and root disease (RD) materials partially overlapped, suggesting that the effects of *R. solanacearum* infection on metabolite levels may be highest in tomato leaves (Figure 4A). A correlation analysis of the multi-tissue metabolome revealed strong correlations among the biological replicates for each tissue, whereas metabolic profiles tended to differ among tissues (Figure S5). Within tissues, LC and LD materials could be distinguished from each other, while this was not true for some RC and RD materials, similar to the results of the PCA (Figure S5). The results of the thermogram analysis visually illustrated the differential accumulation of metabolites among the four groups of materials (Figure 4B). The tissue samples were divided into two large clusters, with significant differences between the LC and RC control materials, reflecting the pattern of spatially differential accumulation of metabolites across tomato tissues, and the variability of metabolic profiles among different tissues was greater than the effect of *R. solanacearum* on the variation of metabolite content.

To investigate the differential metabolites in response to *R. solanacearum* infection, an orthogonal partial least squares-discrimination analysis (OPLS-DA) was performed. The control and susceptible groups (LC vs. LD, and RC vs. RD) were significantly separated on the first principal component with P1 values of 41.0% and 33.0%, respectively (Figure 4C, D). Significance diagnostics showed that R2Y and Q2 values in leaves were 0.997 and 0.996, respectively, while R2Y and Q2 values in roots were 0.995 and 0.990, respectively, neither of which exceeded the true value (horizontal line), implying no overfitting (Figure S6). Differentially accumulated metabolites (DAMs) were identified using Student's *t*-tests and fold changes (P-value < 0.05; fold change > 2 or < 0.5). Volcano plots identified 251 differential metabolites in leaves (214 up-regulated and 37 down-regulated), of which 150 were modified metabolites, and 131 differential metabolites in roots (67 up-regulated and 64 down-regulated), of which 74 were modified metabolites. Further comparing the differential metabolites between tissues (leaves and roots), 45 DAMs were common to both tissues, of which 28 were modified metabolites; 206 and 86 DAMs were specific to leaves and roots, respectively (Figure 4E, F; Table S10). Thus, modified metabolites may play an important role in the tomato response to *R. solanacearum* infestation.

Modified metabolic biomarkers for *R. solanacearum* in tomato

The importance of diagnostic biomarkers for the prevention of *R. solanacearum* was identified, as *R. solanacearum* infestation severely affects the yield of tomato plants (Tans-Kersten et al., 2001; Tian et al., 2021). Using an OPLS-DA model, the 369 and 330 validated differential metabolites

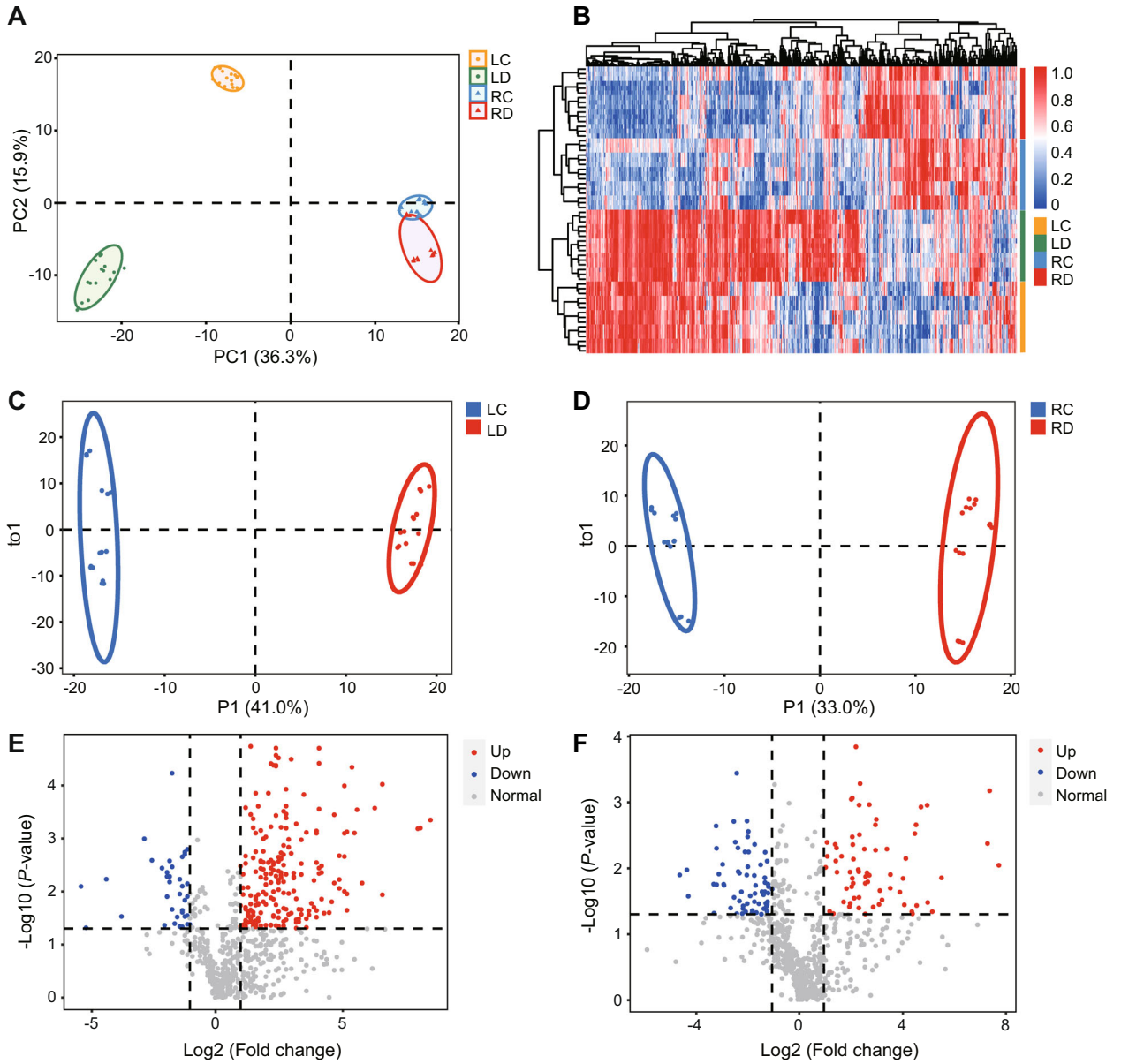

Figure 4. Screening for differentially accumulated metabolites in tomato tissues in response to *Ralstonia solanacearum* infection

(A) Principal component analysis (PCA) based on the relative content of metabolites in different tomato tissues. **(B)** Visualization of hierarchical clustering maps of metabolites detected in different tomato tissues. **(C)** Score plot of the OPLS-DA model based on differences in metabolic levels in tomato leaves. **(D)** Score plot of the OPLS-DA model based on differences in metabolic levels in tomato roots. **(E)** Volcano plot of 251 differentially accumulated metabolites between LC and LD groups (P-value < 0.05; FC, fold change > 2 or <0.5). **(F)** Volcano plot of 131 differentially accumulated metabolites between RC and RD groups (P < 0.05; FC, fold change > 2 or <0.5). LC, leaf control; LD, leaf disease; OPLS-DA, orthogonal partial least squares-discrimination analysis; RC, root control; RD, root diseased.

were further screened for their variable importance in projection (VIP) values greater than 1 in leaves and roots, respectively (Figure 4C, D). Based on univariate and multivariate statistical analyses (fold change; false discovery rate-corrected P-value; VIP value), 13 DAMs were identified in both tissues (Figure 5A; Table S10). Pie charts were used to illustrate the classification of these DAMs, including alkaloids, amino acids, nucleotides, naphthalenes, and phenolamines, among other classes; of these, nine metabolites were labeled as modified metabolites (Figure 5B).

The 13 DAMs were used as a candidate combined biomarker in a binary logistic regression for receiver operating characteristic (ROC) curve analysis (Figure 5C). The ROC curve confirmed good sensitivity of the combined biomarker, as well as high specificity for both susceptible leaf and root materials. The area under the curve (AUC) values were all 1, indicating that the candidate biomarker could clearly discriminate tomatoes infected with *R. solanacearum* from controls. Therefore, these 13 DAMs could be used as a combined biomarker to discriminate between *R. solanacearum*-susceptible

tomatoes and healthy controls. Moreover, the separate analyses of ROC curves were performed for each of the 13 DAMs (Figure S7). All 13 DAMs showed good sensitivity and specificity (AUC > 0.85) in both leaf and root material and could also be used as biomarkers alone to screen for *R. solanacearum* infection. However, compared to the modified metabolites (AUC > 0.90), metabolites without modified groups, such as NL34613 (putrescine), had poor discriminatory ability for leaf materials, with an AUC value of 0.89.

The DAMs were compared across tissues to identify those common to all tissues, as well as those specific to each. In response to *R. solanacearum* infection, several metabolites accumulated in both leaf and/or root tissues, and all six of these metabolites were found to have modified groups (Figure S8). To visualize the differential accumulation patterns of metabolites in tomato after infection with *R. solanacearum*, 26 DAMs were selected, including amino acids, lipids, and phenolamines (the three most abundant substances), and

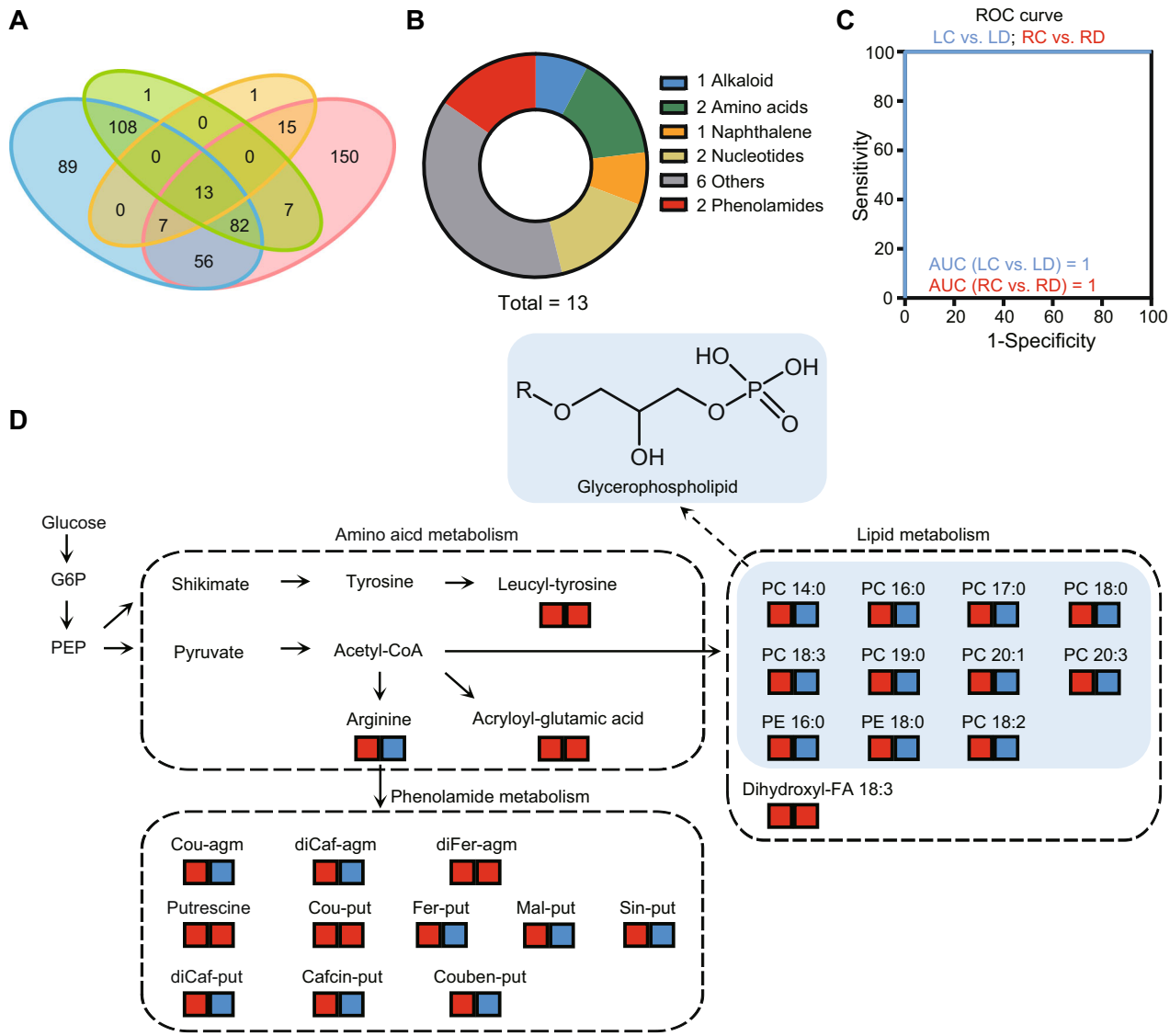

Figure 5. Selection and validation of biomarkers for *Ralstonia solanacearum* infection in tomato

(A) Venn diagrams for screening candidate biomarkers for *R. solanacearum* infection based on univariate and multivariate statistical analyses. Blue and red represent metabolites with variable importance in projection (VIP) values > 1 in leaves and roots, respectively; green and orange represent metabolites with *P*-values < 0.05 (FDR, false discovery rate significance criterion equal to 0.1) and fold changes > 2 or <0.5 in leaves and roots, respectively. **(B)** Pie chart illustrating the classification of the 13 potential biomarkers. **(C)** Validation of a potential combined biomarker consisting of 13 differentially accumulated metabolites based on receiver operating characteristic (ROC) curves. Area under the curve (AUC) = 0.5, it was the same as the follower guess, the model had no predictive value; 0.5 < AUC < 1, it was better than random guessing, and the model had predictive value; AUC = 1, the prediction model could be used to get a perfect prediction. **(D)** The accumulation pattern plot of differentially accumulated metabolites. The small squares represent changes in the relative contents of metabolites in response to *R. solanacearum*. The left squares represent leaves and the right squares represent roots; red represents increases (fold change > 2), and blue represents no significant change (0.5 < fold change < 2). Agm, agmatine; Ben, benzoyl; Cin, cinnamyl; Cou, coumaroyl; Caf, caffeoyl; Fer, feruloyl; Mal, malonyl; Put, putrescine; Sin, sinapoyl.

they were labeled in the metabolic pathway for analysis (Figure 5D). The results showed that the accumulation of all 26 metabolites, including 24 modified metabolites, increased significantly in leaves after infection with *R. solanacearum*, while only six metabolites, including five modified metabolites, increased in roots. In addition, lipids carrying glycerophospholipid moieties and most of the acylated modified phenolamines did not increase in abundance in the roots of diseased plants. Taken together, the accumulation of *R. solanacearum*-modified metabolites increased significantly in infected tomato root and leaf tissues, with a more pronounced increase in leaves. Therefore, various modifying groups of metabolites play an important role in altering the polarity, biological activity and function of metabolites.

DISCUSSION

In plants, metabolite structural and functional diversity is largely determined by chemical modifications of the basic metabolite backbone (Wang et al., 2019). However, current detection methods target only some of the known modification types, and large-scale systematic studies on plant metabolic modifications have not yet been reported (Dai et al., 2014, 2016; Ballet et al., 2018; Li et al., 2019). Therefore, improving detection coverage remains an important challenge for metabolomics (Fernie et al., 2004). In this study, a new WTMM strategy was developed that enables the large-scale acquisition of modified metabolite signals, and MS2T libraries were constructed for the identification and annotation of modified metabolites. The WTMM strategy integrates the high sensitivity of Q-Trap and the high-resolution features of QE, although the metabolic signals they acquire only overlap by a certain percentage, which poses a certain challenge for the structural resolution of metabolites using HRMS data. However, the combination of the two acquisition methods allows for a more comprehensive and systematic acquisition of modified metabolic profiles, which provides additional source data for the discovery of new modified metabolites. More than 34,000 modified metabolic signals were obtained in tomato using the WTMM strategy, providing an important data resource for the discovery of new metabolites and modification types. In addition, the detection of phytohormones (GA4) confirmed the advantageous high sensitivity of the WTMM strategy.

Meanwhile, based on the NL-EPI detection mode, high-quality MS2 information can be obtained for modified metabolites, laying the foundation for subsequent metabolite identification. In this study, a total of 125 modification types and 2,118 metabolites were identified and annotated, among which 165 modified metabolites were identified for the first time in tomato. However, due to the huge amount of information on modified metabolites obtained using the WTMM strategy, the efficiency of manual annotation is too low to meet practical needs. Therefore, the accurate, rapid annotation of modified metabolites will be the focus of future work. Previous studies of plant-modified metabolites have mainly used the QE-Orbitrap method, which detects only a few known types of modified metabolic signals. The WTMM strategy integrates the advantages of Q-Trap and QE-Orbitrap, which not only covers all currently reported modification types, but also detects many unknown NL metabolic signals, which offers the possibility to discover new modification types and identify new modified metabolites. When applying the WTMM strategy, the effects of metabolic sample pretreatment and extraction methods on metabolic signal detection also need to be considered, while positive and negative ion modes should be integrated for simultaneous acquisition of plant-modified metabolic signals. Therefore, the WTMM strategy may be used to detect small but important differences between groups of samples and is more suitable for large-scale quantitative studies of modified metabolites in plant samples. However, the detection of isomers resulting from different positions of the same number and type of modifying groups on the carbon skeleton of metabolites remains a challenge. Meanwhile, with the continuous upgrading of sequencing technology, we can efficiently screen relevant candidate genes for metabolite biosynthesis by integrating genomic, transcriptomic and other multi-omics information, and then resolve the genetic basis for the formation of plant-modified metabolites (Luo, 2015; Zhu et al., 2018).

Applying the WTMM database established in this study to different tomato samples (healthy controls and disease-susceptible samples), a total of 251 DAMs were identified in leaves, including 150 modified metabolites, and 131 DAMs were identified in roots, including 74 modified metabolites. In addition, disease-responsive modified metabolites, such as amino acids, lipids, and phenolic amines, accumulated to a greater extent in tomato root and leaf tissues (Wan et al., 2020). For example, falcarindiol, a typical acetylenic lipid, was shown to have important inhibitory effects on fungal and bacterial pathogens in tomato leaves (Jeon et al., 2020). Based on these results, modified metabolites may act as signals to enhance tomato defense responses.

In summary, the WTMM strategy applies a broad targeting strategy to improve the coverage as well as sensitivity of the assay, combines high-resolution data for accurate annotation of metabolic signals, and is suitable for large-scale quantitative studies of modified metabolites with good reproducibility and linearity. This strategy is applicable to any plant species and is important for the discovery of functional modified metabolites in plants; at the same time, it can also be combined with other omics data to provide potential for in-depth studies on the genetic basis of the synthesis and regulation of plant-modified metabolites.

MATERIALS AND METHODS

Planting materials and growth conditions

Five different varieties of tomato materials (Table S2) used in this study were planted in the greenhouse of Hainan

University, and a control group and an experimental group were set up. The materials in the experimental group were inoculated with *R. solanacearum* by the soil irrigation method, while the materials in the control group were not inoculated. In addition, greenhouse management, including irrigation, fertilization, and pest control, largely followed normal agricultural practices. After 30 d of inoculation with *R. solanacearum*, the leaves and roots of three plants with similar growth status of each variety were selected to prepare mixed samples respectively. Each sample has three biological replicates. The samples were quickly stored in liquid nitrogen and freeze-dried for subsequent metabolite extraction and detection analysis.

Chemicals

Chromatographic-grade methanol, acetonitrile, and acetic acid reagents used in this study were purchased from Merck (Darmstadt, Germany, http://www.merck-chemicals.com). Deionized water was prepared using a LabTower EDI 15 system from Thermo Fisher Scientific (Waltham, MA, USA, https://www. thermofisher.cn). The authentic standards used were purchased from Sigma-Aldrich Company (Saint Louis, MO, USA, http://www.sigmaaldrich.con).

Sample preparation and extraction

The freeze-dried samples were crushed using a mixer mill (MM 400, Retsch, Arzberg, Germany, https://www.retsch.cn/) with a zirconia bead for 1.5 min at 25 Hz. Then, 100 mg of dry powder was weighed and added to 1.0 mL of 70% methanol aqueous solution containing 0.1 mg/L lidocaine, and extracted at 4°C for 10 h. After centrifugation at 10,000 *g* for 10 min at 4°C, the supernatant was filtered through an organic filter (13 mm, 0.2 μm, ValueLab, CA, USA, https://www.agilent.com.cn/) for UHPLC-MS analysis.

Ultra-high performance liquid chromatography detection conditions

The extracted metabolic samples were separated using a UHPLC system (Shimadzu Nexera X2, Kyoto, Japan, www.shimadzu.com.cn/). Analytical conditions were as follows: column, shim-pack GISS C18 (pore size 5.0 μm, length 2 × 150 mm, Shimadzu); mobile phase, water (0.04% acetic acid) and acetonitrile (0.04% acetic acid); elution gradient, water, acetonitrile, 95:5 v/v at 0 min, 5:95 v/v at 10 min, 5:95 v/v at 11 min, 95:5 v/v at 11.1 min, 95:5 v/v at 15 min; flow rate, 0.4 mL/min; temperature, 40°C; injection volume, 2 μL. The UHPLC-separated samples were detected and analyzed by Q-Trap and QE- Orbitrap MS, respectively.

Instrument parameters and data screening

The API 6500 Q-Trap system was equipped with an Electrospray Ionization (ESI) Turbo ion spray interface and was controlled using Analyst 1.6.3 software (AB SCIEX, Framingham, MA, USA, https://sciex.com) to operate in positive ion mode. The main parameters of the ESI source are as follows: ion source temperature 500°C; ion spray voltage (IS) 5500 V; ion source gas I (GSI), ion source gas II (GSII) and curtain gas (CUR) were set at 55, 60, and 25 psi, respectively; collision gas (CAD) was set to high mode. The modified metabolic profile was detected using the NL-EPI mode of the Q-Trap system, in which the neutral loss value starts from 14 Da and takes 1 Da steps, namely NL = 14, NL = 15, NL = 16…, NL = 245, and the precursor ion scan range was set from 19 to 1,000 Da for each NL transition. If the scan reaches the preset NL value (NL = 14–245 Da), and reaches the preset signal intensity to trigger information-dependent acquisition, the linear ion trap module will be activated to perform enhanced product ion scanning to obtain the MS2 spectrum of the precursor ion. The settings of parameters such as product ions, DP and CE were optimized before quantitative analysis, where the ranges of DP and CE were 10–60.

Full MS/dd-MS2 detection mode on the QE platform was performed in positive ion mode with precursor ion scans ranging from 50 to 1,000 Da. The main parameters of the ESI source were as follows: sheath gas 40 psi; auxiliary gas 12 psi; spray voltage 3,000 V; capillary temperature 360°C; S-lens voltage 55 V; auxiliary gas heating temperature 350°C.

Data processing and metabolite characterization

High-resolution raw data were submitted to Compound Discoverer 3.1 software (Thermo Fisher Scientific) for automatically matching to the online database; or after format conversion by Proteowizard (http://proteowizard.sourceforge.net/download.html), submitted to SIRIUS (https://bio.informatik.uni-jena.de/sirius/), MetDNA (http://metdna.zhulab.cn/), MS2 Analyzer (http://fiehnlab.ucdavis.edu/projects/MS2Analyzer/) and other software for auxiliary analysis. Raw data acquired in sMRM mode were subjected to peak areas extraction for metabolite quantification using MultiQuant 3.0.3 software. The criteria for the structural identification of metabolites are categorized into three levels: level 1 is achieved by comparing information such as MS, MS/MS and retention times of standards; level 2 is achieved by manual solving of spectra or by comparing information such as MS, MS/MS, and retention time of published literature and databases; and level 3 is achieved by using high-resolution precursor ion data and incomplete MS/MS to achieve the identification of partial structures or groups (Schymanski et al., 2014). Principal component analysis and OPLS-DA were performed under the Par algorithm of SIMCA 13.0 software. The relative contents of different tissue-modified metabolites were displayed by histogram using GraphPad Prism 8 software, and potential biomarkers in response to bacterial wilt were assessed by ROC curves.

Gaussian graphical modeling

Gaussian graphical modeling, an undirected probabilistic graphical model estimating the conditional dependence between variables, is based on pairwise Pearson's correlation coefficients conditioned against the correlation with all other metabolites (Chen et al., 2016). GeneNet package 1.2.8 (from the CRAN, http://www.cran.r-project.org/) was used to estimate the *P*-correlation and assess the significance of

the edges between metabolites, and the metabolite pairs were used to construct a metabolic network with the software Cytoscape (3.0.2).

ACKNOWLEDGEMENTS

This work was supported by the National Key R&D Program of China (2021YFA0909600), the National Natural Science Foundation of China (No. 32100212, 32101662), the Hainan Province Science and Technology Special Fund (ZDYF2022XDNY144), the Young Elite Scientists Sponsorship Program by CAST (No. 2019QNRC001), the Hainan Provincial Academician Innovation Platform Project (No. HD-YSZX-202004), the Hainan University Startup Fund (No. KYQD (ZR) 21025). We thank the Metabolic Biology Laboratory led by Prof. Jie Luo at Hainan University for help with metabolic analysis.

CONFLICTS OF INTEREST

The authors declare they have no competing financial interests.

AUTHOR CONTRIBUTIONS

S.W. designed the research and supervised this study. J.Y., R.C. and Z.Z. participated in the material preparation. R.C. and W.Y. carried out the metabolite analyses. J.Y., R.C., C. W. and C.L. performed the data analyses. R.C. and W.Y. performed most of the experiments. S.W., J.Y. and R.C. wrote the manuscript. All authors contributed to reviewing and editing of the manuscript. All authors read and approved the contents of this paper.

Edited by: Guodong Wang, Institute of Genetics and Developmental Biology, CAS, China

Received Oct. 7, 2023; **Accepted** Feb. 4, 2024

REFERENCES

Afendi, F.M., Okada, T., Yamazaki, M., Hirai-Morita, A., Nakamura, Y., Nakamura, K., Ikeda, S., Takahashi, H., Altaf-Ul-Amin, M., Darusman, L.K., et al. (2012). KNApSAcK family databases: Integrated metabolite-plant species databases for multifaceted plant research. Plant Cell Physiol. **53:** e1.

Ahmad, M.Z., Zhang, Y., Zeng, X., Li, P., Wang, X., Benedito, V.A., and Zhao, J. (2021). Isoflavone malonyl-CoA acyltransferase GmMaT2 is involved in nodulation of soybean by modifying synthesis and secretion of isoflavones. J. Exp. Bot. **72:** 1349–1369.

Ballet, C., Correia, M.S.P., Conway, L.P., Locher, T.L., Lehmann, L.C., Garg, N., Vujasinovic, M., Deindl, S., Lohr, J.M., and Globisch, D. (2018). New enzymatic and mass spectrometric methodology for the selective investigation of gut microbiota-derived metabolites. Chem. Sci. **9:** 6233–6239.

Chen, L., Huang, X.X., Zhao, S.M., Xiao, D.W., Xiao, L.T., Tong, J.H., Wang, W.S., Li, Y.J., Ding, Z., and Hou, B.K. (2020). IPyA glucosylation mediates light and temperature signaling to regulate auxin-dependent hypocotyl elongation in *Arabidopsis*. Proc. Natl. Acad. Sci. U.S.A. **117:** 6910–6917.

Chen, W., Gong, L., Guo, Z., Wang, W., Zhang, H., Liu, X., Yu, S., Xiong, L., and Luo, J. (2013). A novel integrated method for large-scale detection, identification, and quantification of widely targeted metabolites: Application in the study of rice metabolomics. Mol. Plant **6:** 1769–1780.

Chen, W., Wang, W.S., Peng, M., Gong, L., Gao, Y.Q., Wan, J., Wang, S. C., Shi, L., Zhou, B., Li, Z.M., et al. (2016). Comparative and parallel genome-wide association studies for metabolic and agronomic traits in cereals. Nat. Commun. **7:** 12767.

D'Auria, J.C., and Gershenzon, J. (2005). The secondary metabolism of *Arabidopsis thaliana*: Growing like a weed. Curr. Opin. Plant Biol. **8:** 308–316.

Dai, W., Yin, P., Zeng, Z., Kong, H., Tong, H., Xu, Z., Lu, X., Lehmann, R., and Xu, G. (2014). Nontargeted modification-specific metabolomics study based on liquid chromatography-high-resolution mass spectrometry. Anal. Chem. **86:** 9146–9153.

Dai, W., Tan, J., Lu, M., Xie, D., Li, P., Lv, H., Zhu, Y., Guo, L., Zhang, Y., Peng, Q., et al. (2016). Nontargeted modification-specific metabolomics investigation of glycosylated secondary metabolites in tea (*Camellia sinensis* L.) based on liquid chromatography-high-resolution mass spectrometry. J. Agric. Food Chem. **64:** 6783–6790.

De Vos, R.C., Moco, S., Lommen, A., Keurentjes, J.J., Bino, R.J., and Hall, R.D. (2007). Untargeted large-scale plant metabolomics using liquid chromatography coupled to mass spectrometry. Nat. Protoc. **2:** 778–791.

Fang, C.Y., Fernie, A.R., and Luo, J. (2019). Exploring the diversity of plant metabolism. Trends Plant Sci. **24:** 83–98.

Fang, H., Shen, S., Wang, D., Zhang, F., Zhang, C., Wang, Z., Zhou, Q., Wang, R., Tao, H., He, F., et al. (2021). A monocot-specific hydroxycinnamoylputrescine gene cluster contributes to immunity and cell death in rice. Sci. Bull. **66:** 2381–2393.

Fernie, A.R., Trethewey, R.N., Krotzky, A.J., and Willmitzer, L. (2004). Metabolite profiling: From diagnostics to systems biology. Nat. Rev. Mol. Cell Biol. **5:** 763–769.

Frydman, A., Liberman, R., Huhman, D.V., Carmeli-Weissberg, M., Sapir-Mir, M., Ophir, R., W. Sumner, L., and Eyal, Y. (2013). The molecular and enzymatic basis of bitter/non-bitter flavor of citrus fruit: Evolution of branch-forming rhamnosyltransferases under domestication. Plant J. **73:** 166–178.

Frydman, A., Weisshaus, O., Bar-Peled, M., Huhman, D.V., Sumner, L.W., Marin, F.R., Lewinsohn, E., Fluhr, R., Gressel, J., and Eyal, Y. (2004). Citrus fruit bitter flavors: isolation and functional characterization of the gene Cm1,2RhaT encoding a 1,2 rhamnosyltransferase, a key enzyme in the biosynthesis of the bitter flavonoids of citrus. Plant J. **40:** 88–100.

Gandia-Herrero, F., and Garcia-Carmona, F. (2013). Biosynthesis of betalains: Yellow and violet plant pigments. Trends Plant Sci. **18:** 334–343.

Garagounis, C., Delkis, N., and Papadopoulou, K.K. (2021). Unraveling the roles of plant specialized metabolites: Using synthetic biology to design molecular biosensors. New Phytol. **231:** 1338–1352.

Itkin, M., Heinig, U., Tzfadia, O., Bhide, A.J., Shinde, B., Cardenas, P. D., Bocobza, S.E., Unger, T., Malitsky, S., Finkers, R., et al. (2013). Biosynthesis of antinutritional alkaloids in solanaceous crops is mediated by clustered genes. Science **341:** 175–179.

Jeon, J.E., Kim, J.G., Fischer, C.R., Mehta, N., Dufour-Schroif, C., Wemmer, K., Mudgett, M.B., and Sattely, E. (2020). A pathogen-responsive gene cluster for highly modified fatty acids in tomato. Cell **180:** 176–187 e119.

Keenan, E.K., Zachman, D.K., and Hirschey, M.D. (2021). Discovering the landscape of protein modifications. Mol. Cell **81:** 1868–1878.

Li, H., Qin, Q., Shi, X., He, J., and Xu, G. (2019). Modified metabolites mapping by liquid chromatography-high resolution mass spectrometry using full scan/all ion fragmentation/neutral loss acquisition. J. Chromatogr. A **1583:** 80–87.

Li, Y., Leveau, A., Zhao, Q., Feng, Q., Lu, H., Miao, J., Xue, Z., Martin, A. C., Wegel, E., Wang, J., et al. (2021). Subtelomeric assembly of a multi-gene pathway for antimicrobial defense compounds in cereals. Nat. Commun. **12:** 2563.

Luo, J. (2015). Metabolite-based genome-wide association studies in plants. Curr. Opin. Plant Biol. **24:** 31–38.

Lv, W., Wang, L., Xuan, Q., Zhao, X., Liu, X., Shi, X., and Xu, G. (2020). Pseudotargeted method based on parallel column two-dimensional liquid chromatography-mass spectrometry for broad coverage of metabolome and lipidome. Anal. Chem. **92:** 6043–6050.

Ono, E., Fukuchi-Mizutani, M., Nakamura, N., Fukui, Y., Yonekura-Sakakibara, K., Yamaguchi, M., Nakayama, T., Tanaka, T., Kusumi, T., and Tanaka, Y. (2006). Yellow flowers generated by expression of the aurone biosynthetic pathway. Proc. Natl. Acad. Sci. U.S.A. **103:** 11075–11080.

Reinders, J., and Sickmann, A. (2007). Modificomics: Posttranslational modifications beyond protein phosphorylation and glycosylation. Biomol. Eng. **24:** 169–177.

Saito, K., and Matsuda, F. (2010). Metabolomics for functional genomics, systems biology, and biotechnology. Annu. Rev. Plant Biol. **61:** 463–489.

Schymanski, E.L., Jeon, J., Gulde, R., Fenner, K., Ruff, M., Singer, H.P., and Hollender, J. (2014). Identifying small molecules via high resolution mass spectrometry: Communicating confidence. Environ. Sci. Technol. **48:** 2097–2098.

Shen, S., Wang, S., Yang, C., Wang, C., Zhou, Q., Zhou, S., Zhang, R., Li, Y., Wang, Z., Dai, L., et al. (2023). Elucidation of the melitidin biosynthesis pathway in pummelo. J. Integr. Plant Biol. **65:** 2505–2518.

Shi, X.J., Yang, W.Z., Qiu, S., Yao, C.L., Shen, Y., Pan, H.Q., Bi, Q.R., Yang, M., Wu, W.Y., and Guo, D.A. (2017). An in-source multiple collision-neutral loss filtering based nontargeted metabolomics approach for the comprehensive analysis of malonyl-ginsenosides from *Panax ginseng*, *P. quinquefolius*, and *P. notoginseng*. Anal. Chim. Acta **952:** 59–70.

Singh, G., Agrawal, H., and Bednarek, P. (2023). Specialized metabolites as versatile tools in shaping plant–microbe associations. Mol. Plant **16:** 122–144.

Sonawane, P.D., Heinig, U., Panda, S., Gilboa, N.S., Yona, M., Kumar, S.P., Alkan, N., Unger, T., Bocobza, S., Pliner, M., et al. (2018). Short-chain dehydrogenase/reductase governs steroidal specialized metabolites structural diversity and toxicity in the genus Solanum. Proc. Natl. Acad. Sci. U.S.A. **115:** E5419–E5428.

Szymanski, J., Bocobza, S., Panda, S., Sonawane, P., Cardenas, P.D., Lashbrooke, J., Kamble, A., Shahaf, N., Meir, S., Bovy, A., et al. (2020). Analysis of wild tomato introgression lines elucidates the genetic basis of transcriptome and metabolome variation underlying fruit traits and pathogen response. Nat. Genet. **52:** 1111–1121.

Tanaka, Y., Sasaki, N., and Ohmiya, A. (2008). Biosynthesis of plant pigments: anthocyanins, betalains and carotenoids. Plant J. **54:** 733–749.

Tans-Kersten, J., Huang, H., and Allen, C. (2001). Ralstonia solanacearum needs motility for invasive virulence on tomato. J. Bacteriol. **183:** 3597–3605.

Tian, J.-H., Rao, S., Gao, Y., Lu, Y., and Cai, K.-Z. (2021). Wheat straw biochar amendment suppresses tomato bacterial wilt caused by Ralstonia solanacearum: Potential effects of rhizosphere organic acids and amino acids. J. Integr. Agr. **20:** 2450–2462.

Tieman, D., Zeigler, M., Schmelz, E., Taylor, M.G., Rushing, S., Jones, J.B., and Klee, H.J. (2010). Functional analysis of a tomato salicylic acid methyl transferase and its role in synthesis of the flavor volatile methyl salicylate. Plant J. **62:** 113–123.

Tolstikov, V.V., and Fiehn, O. (2002). Analysis of highly polar compounds of plant origin: Combination of hydrophilic interaction chromatography and electrospray ion trap mass spectrometry. Anal. Biochem. **301:** 298–307.

Wan, X., Wu, S., Li, Z., An, X., and Tian, Y. (2020). Lipid metabolism: Critical roles in male fertility and other aspects of reproductive development in plants. Mol. Plant **13:** 955–983.

Wang, S., Alseekh, S., Fernie, A.R., and Luo, J. (2019). The structure and function of major plant metabolite modifications. Mol. Plant **12:** 899–919.

Wang, S., Qiang, Q., Xiang, L., Fernie, A.R., and Yang, J. (2023). Targeted approaches to improve tomato fruit taste. Horticult. Res. **10:** 1–12.

Wang, S., Shen, S., Wang, C., Wang, X., Yang, C., Zhou, S., Zhang, R., Zhou, Q., Yu, H., Guo, H., et al. (2023). A metabolomics study in citrus provides insight into bioactive phenylpropanoid metabolism. Horticult. Res **11:** uhad267.

Wang, Z.L., Gao, H.M., Wang, S., Zhang, M., Chen, K., Zhang, Y.Q., Wang, H.D., Han, B.Y., Xu, L.L., Song, T.Q., et al. (2020). Dissection of the general two-step di-*C*-glycosylation pathway for the biosynthesis of (iso)schaftosides in higher plants. Proc. Natl. Acad. Sci. U.S.A. **117:** 30816–30823.

Wen, W., Li, D., Li, X., Gao, Y., Li, W., Li, H., Liu, J., Liu, H., Chen, W., Luo, J., et al. (2014). Metabolome-based genome-wide association study of maize kernel leads to novel biochemical insights. Nat. Commun. **5:** 3438.

Weng, J.K., Lynch, J.H., Matos, J.O., and Dudareva, N. (2021). Adaptive mechanisms of plant specialized metabolism connecting chemistry to function. Nat. Chem. Biol. **17:** 1037–1045.

Wu, J., Zhu, W., Shan, X., Liu, J., Zhao, L., and Zhao, Q. (2022). Glycosides-specific metabolomics combined with precursor isotopic labeling for characterizating plant glycosyltransferases. Mol. Plant **15:** 1517–1532.

Xia, J., Guo, Z., Yang, Z., Han, H., Wang, S., Xu, H., Yang, X., Yang, F., Wu, Q., Xie, W., et al. (2021). Whitefly hijacks a plant detoxification gene that neutralizes plant toxins. Cell **184:** 1693–1705 e1617.

Yan, J., Li, H., Li, Y., Zhang, N., and Zhang, S. (2022). Abscisic acid synthesis and root water uptake contribute to exogenous methyl jasmonate-induced improved tomato drought resistance. Plant Biotechnol. Rep. **16:** 183–193.

Yang, C., Shen, S., Zhou, S., Li, Y., Mao, Y., Zhou, J., Shi, Y., An, L., Zhou, Q., Peng, W., et al. (2022). Rice metabolic regulatory network spanning the entire life cycle. Mol. Plant **15:** 258–275.

Zhang, G.Z., Jin, S.H., Jiang, X.Y., Dong, R.R., Li, P., Li, Y.J., and Hou, B.K. (2016). Ectopic expression of UGT75D1, a glycosyltransferase preferring indole-3-butyric acid, modulates cotyledon development and stress tolerance in seed germination of *Arabidopsis thaliana*. Plant Mol. Biol. **90:** 77–93.

Zhang, W., Wang, S., Yang, J., Kang, C., Huang, L., and Guo, L. (2022). Glycosylation of plant secondary metabolites: Regulating from chaos to harmony. Environ. Exp. Bot. **194:** 104703.

Zheng, F., Zhao, X., Zeng, Z., Wang, L., Lv, W., Wang, Q., and Xu, G. (2020). Development of a plasma pseudotargeted metabolomics method based on ultra-high-performance liquid chromatography-mass spectrometry. Nat. Protoc. **15:** 2519–2537.

Zhong, Y., Xue, X., Liu, Z., Ma, Y., Zeng, K., Han, L., Qi, J., Ro, D.K., Bak, S., Huang, S., et al. (2017). Developmentally regulated glucosylation of bitter triterpenoid in cucumber by the UDP-glucosyltransferase UGT73AM3. Mol. Plant **10:** 1000–1003.

Zhu, G., Wang, S., Huang, Z., Zhang, S., Liao, Q., Zhang, C., Lin, T., Qin, M., Peng, M., Yang, C., et al. (2018). Rewiring of the fruit metabolome in tomato breeding. Cell **172:** 249–261 e212.

SUPPORTING INFORMATION

Additional Supporting Information may be found online in the supporting information tab for this article: http://onlinelibrary.wiley.com/doi/10.1111/jipb.13629/suppinfo

Figure S1. Detailed structural annotation workflow for modified metabolites based on MS2 Analyzer software
Figure S2. Construction of a metabolic reaction network based on MetDNA algorithm for metabolite annotation
Figure S3. Annotation of novel modified metabolites in tomato combined with high-resolution mass spectrometry data
Figure S4. Summary of the main types of modifications to flavonoid structures
Figure S5. Correlation analysis of the metabolome of different tomato tissues
Figure S6. The evaluation plots of Orthogonal Partial Least Squares Discrimination Analysis
Figure S7. Assessment of potential biomarkers based on receiver operating characteristic curves
Figure S8. The histograms based on the relative content of differentially accumulated metabolites in tomato leaves and roots

Table S1. Metabolite reporting checklist
Table S2. The information of five tomato accessions used in this study
Table S3. The (almost) non-redundant MS2 spectral tag (MS2T) library of tomato obtained by the stepwise neutral loss-enhanced product ion (NL-EPI) method
Table S4. The annotation results of MS2 spectral tag (MS2T) library
Table S5. The information of modifying groups based on MS2 Analyzer software
Table S6. The annotation result based on MetDNA software
Table S7. One hundred and twenty-five metabolite modifications detected in tomato
Table S8. Validation of method reproducibility and linearity
Table S9. Data matrix of 826 metabolites of tomato materials. LC, leaf control; LD, leaf disease; RC, root control; RD, root diseased. Three biological replicates were used for analysis
Table S10. The statistical results of 724 metabolites (metabolites with N/A data were filtered out). FDR, false discovery rate; LC, leaf control; LD, leaf disease; RC, root control; RD, root diseased; VIP, variable important in projection

Scan using WeChat with your smartphone to view JIPB online

Scan with iPhone or iPad to view JIPB on Twitter